



LETTERS TO THE EDITOR

Normal Global Longitudinal Strain

An Individual Patient Meta-Analysis



There is abundant evidence of the prognostic and diagnostic value of global longitudinal strain (GLS). However, despite multiple reports, uncertainty persists about the variance in normal GLS. The difficulties in defining the lower limit of normality (LLN) have provided 1 reason for slow uptake of GLS into current clinical guidelines. This individual, adult-patient meta-analysis sought to define the distribution of normal GLS and LLN.

PubMed, Cochrane, and EMBASE were searched through August 2018 using the keywords “left ventricle,” “normal global longitudinal strain,” and “speckle tracking echocardiography,” including all relevant synonyms. Relevant results before 2011 were excluded because papers up until this date had been previously included in a GLS meta-analysis (1) and speckle tracking software has significantly evolved. Studies were included if they included at least 20 healthy (defined as lack of known disease) individuals >18 years of age, reported speckle tracking-based GLS, and had contact information available. In the case where the contacted authors offered unpublished data that met the original inclusion criteria, this was included. Variable distributions were assessed using histograms, and data were presented as median [25th centile, 75th centile]. Standard linear regression was used to determine associations of GLS; variables found to be colinear were removed from the regression. One-way analysis of variance followed by pairwise comparison with a Bonferroni correction was used to compare means between vendors. The 5th percentile was used to indicate the LLN. Traditional meta-analysis techniques were used to define the scope of responder and publication bias.

Of 1,084 PubMed results, 76 abstracts were reviewed, 56 papers were assessed, and 16 were included. No additional papers were identified in the Cochrane or EMBASE reviews. Using a conventional meta-analysis approach from the 16 included papers, the mean GLS was 20.7 (standard error = 0.04), with only minor funnel plot asymmetry, arguing against significant bias.

Individual data were received from 8 of the 16 eligible papers (2-9), composing 2,396 people of mean

age 42 years (range: 18 to 92 years), weight 66 ± 12 kg, height 169 ± 9 cm, body surface area 1.7 ± 0.2 m², and systolic blood pressure 120 ± 13 mm Hg. In the interest of simplicity, GLS was expressed without a positive or negative number. The normal range for GLS was 21.0 [19.2, 22.7] but varied significantly with age (Figure 1). GLS was lower in patients older than age 60 years when compared with patients younger than age 60 years (20.0% [18.4, 21.9] vs 21.0% [19.4, 22.9], $p < 0.01$). GLS <16% was present in 66 people (2.8%); mean age was 54.3 years.

Normal ranges for GLS vary with common clinical covariates such as age (Figure 1), weight ($\beta = -0.03$, $p < 0.01$), systolic blood pressure ($\beta = -0.02$, $p < 0.01$), and non-General Electric platform. The normal range for GLS varied between the vendors, with TomTec presenting the highest values ($n = 644$; 22.1% [20.1, 23.8] , LLN 18.0%), followed by General Electric ($n = 1,013$; 21.2% [19.9, 22.8], LLN 18.2%), Toshiba ($n = 278$; 19.9% [18.3, 21.5], LLN 15.8%), Philips ($n = 379$; 19.6% [18.1, 21.3], LLN 15.5%), and Siemens ($n = 82$; 16.9% [16.0, 18.8], LLN 14.0%), differences being statistically significant (1-way analysis of variance $p < 0.01$). GLS with TomTec was significantly higher than all other vendors ($p < 0.01$ for all 4 comparisons), GE was significantly higher than Toshiba, Philips, and Siemens ($p < 0.01$ for all 3 comparisons). Toshiba ($p < 0.01$) and Philips ($p < 0.01$) were significantly higher than Siemens. Regardless of vendor or clinical covariate, a GLS <16% likely indicates significant myocardial dysfunction.

This is the first study to reliably define GLS variance in a normal population and may now support the routine use of GLS as a clinical decision-making tool. The current results may be unreliable in older populations because it is difficult to reliably exclude all forms of cardiac disease with the screening investigations used in most of the included studies. We hope that the reported values may guide the clinician in detecting myocardial dysfunction.

Nicholas D'Elia, BMSci (Hons) MBBS, GDiP

Stefano Caselli, MD, PhD

Wojciech Kosmala, MD, PhD

Patrizio Lancellotti, MD, PhD

Daniel Morris, MD

Denisa Muraru, MD, PhD

Masaaki Takeuchi, MD, PhD

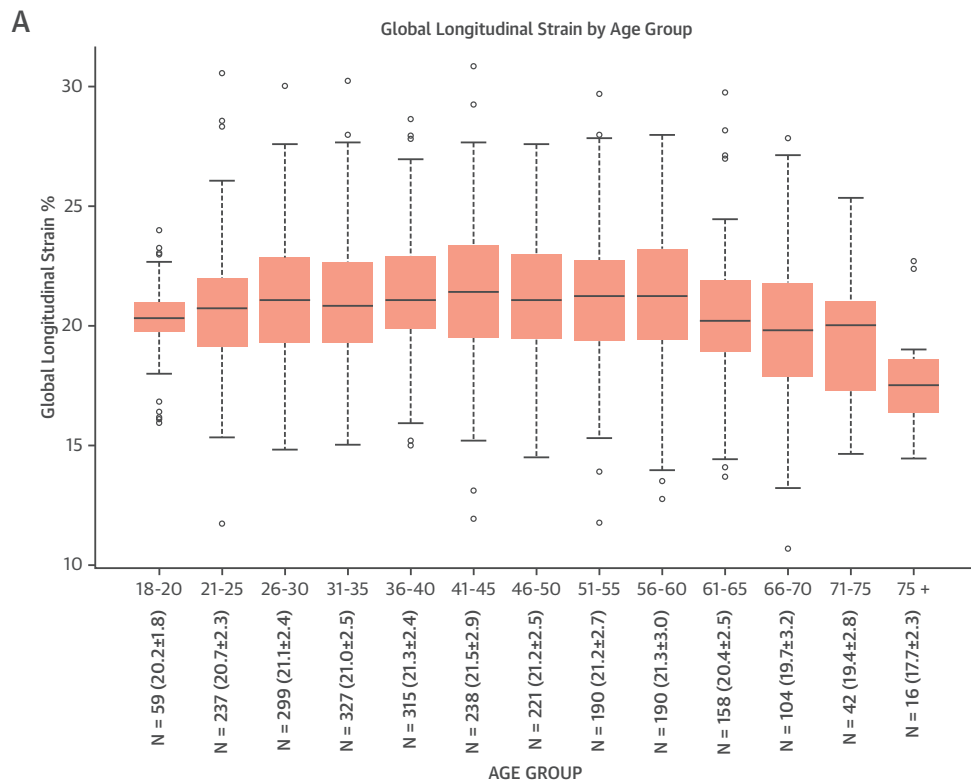
Annemien van den Bosch, MD, PhD

Roderick W.J. van Grootel, MS

Hector Villarraga, MD

Thomas H. Marwick, MBBS, PhD, MPH*

FIGURE 1 Variations of GLS in Normal Individuals



Study Name	Statistics for Each Study					Mean and 95% CI
	Mean	Standard Error	Variance	Lower Limit	Upper Limit	
Reckefuss	20.600	0.217	0.047	20.175	21.025	
Nottin	16.700	0.514	0.265	15.692	17.708	
Takigiku	21.300	0.115	0.013	21.074	21.526	
Takigiku	18.900	0.138	0.019	18.630	19.170	
Takigiku	19.900	0.131	0.017	19.644	20.156	
Fine	17.300	0.183	0.034	16.941	17.659	
Marharaj	17.280	0.293	0.086	16.706	17.854	
Kaya	20.580	0.622	0.386	19.362	21.798	
Kockabay	21.500	0.127	0.016	21.251	21.749	
Moris	21.230	0.113	0.013	21.009	21.451	
Caselli	19.400	0.325	0.106	18.762	20.038	
Charfeddi	22.990	0.519	0.269	21.973	24.007	
Cheng	22.000	0.147	0.022	21.712	22.288	
Cheng	20.200	0.166	0.028	19.874	20.526	
Cong	20.340	0.542	0.294	19.277	21.403	
Eun	17.300	0.539	0.290	16.245	18.355	
Menting	20.800	0.161	0.026	20.485	21.115	
Sugimoto	22.500	0.115	0.013	22.274	22.726	
Kotwica	22.000	0.372	0.138	21.271	22.729	
Total	20.166	0.348	0.121	19.484	20.848	

(A) Boxplot for global longitudinal strain (GLS) for multiple age groups. GLS decreases with age. The ranges for each age group are based on a pooled vendor analysis, and the application of these values in the clinic hence requires clinical judgment. The center bar of the boxplot represents the median value, the extremities of the box represent the first and third quartile, and the whiskers extend to the furthest data point within 1.5 × the interquartile range from the upper and lower limits of the box. Any value outside of this is classified as an outlier. N = number of patients in each group; mean ± standard deviation are indicated in brackets. CI = confidence interval. **(B)** Mean, variance, and upper and lower limits of the studies included in this meta-analysis.

*Baker Heart and Diabetes Institute
75 Commercial Road
Melbourne, Victoria, 3004
Australia
E-mail: tom.marwick@baker.edu.au

<https://doi.org/10.1016/j.jcmg.2019.07.020>

© 2020 by the American College of Cardiology Foundation. Published by Elsevier.

Please note: Dr. Marwick has received research grant support from GE Medical Systems, unrelated to this paper. All other authors have reported that they have no relationships relevant to the contents of this paper to disclose. Jagat Narula, MD, was Guest Editor on this paper.

REFERENCES

1. Yingchoncharoen T, Agarwal S, Popovic ZB, Marwick TH. Normal ranges of left ventricular strain: a meta-analysis. *J Am Soc Echocardiogr* 2013;26:185-91.
2. Caselli S, Montesanti D, Autore C, et al. Patterns of left ventricular longitudinal strain and strain rate in Olympic athletes. *J Am Soc Echocardiogr* 2015; 28:245-53.
3. Sugimoto T, Dulgheru R, Bernard A, et al. Echocardiographic reference ranges for normal left ventricular 2D strain: results from the EACVI NORRE study. *Eur Heart J Cardiovasc Imaging* 2017;18:833-40.
4. Kotwica T, Relewicz J, Rojek A, et al. Role of galectin-3 in subclinical myocardial impairment in psoriasis. *J Eur Acad Dermatol Venereol* 2019;33:136-42.
5. Takigiku K, Takeuchi M, Izumi C, et al. Normal range of left ventricular 2-dimensional strain: Japanese Ultrasound Speckle Tracking of the Left Ventricle (JUSTICE) study. *Circ J* 2012;76:2623-32.
6. Kocabay G, Muraru D, Peluso D, et al. Normal left ventricular mechanics by two-dimensional speckle-tracking echocardiography. Reference values in healthy adults. *Rev Esp Cardiol* 2014;67:651-8.
7. Morris DA, Otani K, Bekfani T, et al. Multidirectional global left ventricular systolic function in normal subjects and patients with hypertension: multicenter evaluation. *J Am Soc Echocardiogr* 2014;27:493-500.
8. Menting ME, McGhie JS, Koopman LP, et al. Normal myocardial strain values using 2D speckle tracking echocardiography in healthy adults aged 20 to 72 years. *Echocardiogr* 2016;33:1665-75.
9. Fine NM, Shah AA, Han IV, et al. Left and right ventricular strain and strain rate measurement in normal adults using velocity vector imaging: an assessment of reference values and intersystem agreement. *Int J Card Imaging* 2013; 29:571-80.

Relationship of Anticoagulant Therapies on Coronary Plaque Progression



A Longitudinal CTA Analysis

Possible antithrombotic effects of anticoagulants in coronary artery disease (CAD) have been proposed, with experimental and clinical data indicating a key role of coagulation factors in the progression of atherosclerosis. Although vitamin K antagonists (VKA) have been associated with increased coronary artery calcification, experimental and clinical data on the effect of direct oral anticoagulants (DOACs) suggest a beneficial influence (1); therefore, we sought to evaluate the effect of different oral anticoagulation agents on the progression of atherosclerosis.

We included consecutive patients between 2006 and 2017 who underwent repeated computed tomography angiography (CTA) before left atrial

catheter ablation of atrial fibrillation (AF). All patients had documented AF (82.0% paroxysmal, 18.0% persistent), but no history of CAD or relevant comorbidities (including valvular pathologies more than mild, reduced ejection fraction more than mild, chemotherapy, or chest radiation). The patients were stratified according to their anticoagulation treatment into controls (no anticoagulation or aspirin), DOAC (all agents), and VKA (time in therapeutic range $\geq 70\%$). Patients with a change in anticoagulation during the observation period or within 6 months before the initial ablation were excluded.

For comparison between the groups, patients were matched using a near-neighbor propensity score (caliper 0.2) for age, sex, and major cardiovascular risk factors (hypercholesterolemia, hypertension, diabetes, smoking, and positive family history for CAD). These factors were again compared at follow-up and showed no significant alterations.

All CT examinations were performed with a standardized protocol including coronary calcium scoring (CCS) followed by contrast-enhanced CTA. AF rate during the scan was 21.7% at baseline and 26.0% at follow-up without differences between the groups ($p = 0.76$ and $p = 0.53$, respectively). Patients with any nondiagnostic segments were excluded. Every segment was analyzed using a dedicated software (QAngio, Medis Medical Imaging Systems, the Netherlands) allowing semi-automated quantification of total plaque volume, stenosis average, plaque thickness, and lesion length. All measurements were performed by 2 experienced, independent observers blinded to patient details.

Of 606 enrolled patients, 161 had repeated CT examinations (mean time interval between scans 3.2 years, $p = 0.12$ between groups) and were included in the analysis. Of these, 61 were control patients, 50 administered DOAC (31 rivaroxaban, 10 dabigatran, 6 apixaban, and 3 edoxaban), and 50 administered VKA. The final groups were comparable at baseline, particularly quantitative plaque analysis; therefore, repeated propensity score matching was not necessary.

Automated lesion analysis revealed an absolute plaque burden progression of $66.5 \pm 136.7 \text{ mm}^3$ in VKA, $27.2 \pm 73.6 \text{ mm}^3$ in controls and an inhibition in DOAC users with $-7.1 \pm 42.1 \text{ mm}^3$ ($p < 0.001$). This translates into an annual progression of $23.2 \pm 47.0 \text{ mm}^3$ for patients administered VKA, $12.3 \pm 4.3 \text{ mm}^3$ for control patients, and $-4.6 \pm 22.9 \text{ mm}^3$ for DOAC users ($p = 0.003$). Average plaque thickness increased by $0.5 \pm 0.7 \text{ mm}$ for VKA, by $0.2 \pm 0.7 \text{ mm}$ in controls, and remained equal with $0.0 \pm 0.34 \text{ mm}$ for DOAC ($p < 0.0001$) (Figure 1). Maximal stenosis